



**HAL**  
open science

## Coordination of hamstrings is individual specific and is related to motor performance

Simon Avrillon, Gaël Guilhem, Aude Barthelemy, François Hug

► **To cite this version:**

Simon Avrillon, Gaël Guilhem, Aude Barthelemy, François Hug. Coordination of hamstrings is individual specific and is related to motor performance. *Journal of Applied Physiology*, 2018, 125 (4), pp.1069-1079. 10.1152/jappphysiol.00133.2018 . hal-02983807

**HAL Id: hal-02983807**

**<https://insep.hal.science//hal-02983807>**

Submitted on 30 Oct 2020

**HAL** is a multi-disciplinary open access archive for the deposit and dissemination of scientific research documents, whether they are published or not. The documents may come from teaching and research institutions in France or abroad, or from public or private research centers.

L'archive ouverte pluridisciplinaire **HAL**, est destinée au dépôt et à la diffusion de documents scientifiques de niveau recherche, publiés ou non, émanant des établissements d'enseignement et de recherche français ou étrangers, des laboratoires publics ou privés.



27 **ABSTRACT (247 words)**

28 The torque sharing strategies between synergist muscles may have important functional  
29 consequences. This study involved two experiments. The first experiment (n=22) aimed: i) to  
30 determine the relationship between the distribution of activation and the distribution of  
31 torque-generating capacity among the heads of the hamstring, and ii) to describe individual  
32 torque-sharing strategies and to determine whether these strategies are similar between legs.  
33 The second experiment (n=35) aimed to determine whether the distribution of activation  
34 between the muscle heads affects the endurance performance during a sustained submaximal  
35 knee flexion task. Surface electromyography (EMG) was recorded from biceps femoris (BF),  
36 semimembranosus (SM), and semitendinosus (ST) during submaximal isometric knee  
37 flexions. Torque-generating capacity was estimated by measuring muscle volume, fascicle  
38 length, pennation angle and moment arm. The product of the normalized EMG amplitude and  
39 the torque-generating capacity was used as an index of muscle torque. The distributions of  
40 muscle activation and of torque-generating capacity were not correlated significantly (all  
41  $P>0.18$ ). Thus, there was a torque imbalance between the muscle heads (ST torque > BF and  
42 SM torque;  $P<0.001$ ), the magnitude of which varied greatly between participants. A  
43 significant negative correlation was observed between the imbalance of activation across the  
44 hamstring muscles and the time to exhaustion ( $P<0.001$ ), i.e. the larger the imbalance of  
45 activation across muscles, the lower the muscle endurance performance. Torque-sharing  
46 strategies between the heads of the hamstrings are individual-specific and related to muscle  
47 endurance performance. Whether these individual strategies play a role in hamstring injury  
48 remains to be determined.

49

50 **NEW & NOTEWORTHY:**

- 51 • The distribution of activation among the heads of the hamstring is not related to the  
52 distribution of torque-generating capacity.
- 53 • The torque-sharing strategies within hamstring muscles vary greatly between  
54 individuals but are similar between legs.
- 55 • Hamstring coordination affects endurance performance; i.e. the larger the imbalance  
56 of activation across the muscle heads, the lower the muscle endurance.

57

58 **KEYWORDS:**

59 Hamstring; Individual coordination; Muscle torque; Muscle endurance

60

61

62

63

64

65

## 66 1. INTRODUCTION

67 Muscle coordination is defined as the distribution of muscle force/torque (rather than just  
68 activation) among individual muscles to produce a given motor task (15). As the number of  
69 muscles exceeds the dimensionality of most tasks, many different coordination strategies are  
70 *theoretically possible* to achieve the same goal. In this way, Hug and Tucker (15)  
71 hypothesized that each individual has unique muscle coordination strategies that will have  
72 specific mechanical effects on his/her musculoskeletal system. To test this hypothesis, it is  
73 necessary to consider the torque produced by individual muscles instead of activation alone.  
74 Muscle torque depends on both the muscle activation and several biomechanical factors (e.g.,  
75 physiological cross-sectional area [PCSA], specific tension, moment arm, and force–length  
76 and force–velocity relationships). When considering muscles with similar specific tension  
77 during an isometric task, an index of torque can be estimated from the muscle activation,  
78 PCSA and moment arm. Using this approach, Hug et al. (14) highlighted large interindividual  
79 differences in the balance of force between the *vastus lateralis* (VL) and the *vastus medialis*  
80 (VM). Specifically, during an isometric knee extension at 20% of the maximal voluntary  
81 contraction (MVC), the VL/VM ratio of the index of force ranged from 38.4 to 84.0%. This  
82 variability resulted from individual differences in both muscle activation and PCSA.  
83 The balance of torque between synergist muscles may have important functional  
84 consequences. For example, using an indirect index of muscle activity (functional Magnetic  
85 Resonance Imaging [fMRI]), Schuermans et al. (34, 35) highlighted the possible role of  
86 altered coordination between the heads of the hamstring in risk of injury. Interestingly, a large  
87 inter-individual variability in PCSA of individual heads of the hamstring has been observed  
88 both in cadavers (coefficient of variation [CV]: 33.3% [biceps femoris short head, BFsh] to  
89 42.4% [biceps femoris long head, BFlh] (42)) and active people (CV: 40.6% for BFlh (36)). It  
90 is unknown whether muscle activation and/or muscle moment arm counteract these individual

91 differences in PCSA such that the distribution of torque among the muscle heads is similar  
92 between individuals.

93 In addition to their possible role in the risk of injury, muscle coordination strategies might  
94 impact muscle performance, as was suggested indirectly by Schuermans et al. (34, 35). Let us  
95 consider two synergist muscles (A and B) during a sustained isometric task at 20% MVC  
96 maintained until exhaustion. During such a task, the muscle endurance performance can be  
97 estimated by the time to exhaustion (16). There are two scenarios for the distribution of  
98 activation during this task: i) A and B are both activated at about 20% of their maximal  
99 activation, i.e. activation is equally shared between muscles, or ii) there is an imbalanced  
100 activation between A and B, in which case one muscle will necessarily be activated at a  
101 higher level than that requested by the task, e.g., A is activated at 30% and B at 10%. In the  
102 latter case, and in the absence of substantial change in activation strategy during the task, it is  
103 likely that muscle A would develop fatigue earlier and this, in turn, would lead to a shorter  
104 time to exhaustion, reflective of lower performance.

105 This study involved two experiments. The aims of the first experiment were: i) to determine  
106 the relationship between the distribution of activation and the distribution of torque-  
107 generating capacity among the heads of the hamstring, and ii) to describe individual torque-  
108 sharing strategies and to determine whether these strategies are similar between legs. To  
109 address these two aims, muscle activation was estimated using electromyography (EMG)  
110 during submaximal isometric knee flexion tasks at 20% of MVC. The between-day reliability  
111 of the activation distribution between the muscle heads was first assessed to test the  
112 robustness of the activation strategies. Muscle torque-generating capacity was estimated by  
113 measurements of the muscle PCSA and moment arm. The second experiment aimed to  
114 determine whether the distribution of activation between the muscle heads affects the  
115 endurance performance during a sustained submaximal task.

## 116 2. METHODS

### 117 2.1. Participants

118 Twenty-two healthy volunteers (age  $24 \pm 2$  yr, weight  $65 \pm 10$  kg, height  $173 \pm 8$  cm; 11  
119 females/11 males) participated in experiment I. In addition to these 22 participants, 13  
120 additional participants were included in experiment II such that a total of 35 healthy  
121 volunteers participated in experiment II (age  $24 \pm 3$  yr, weight  $66 \pm 11$  kg, height  $173 \pm 9$  cm;  
122 16 females/19 males). Participants had no history of hamstring strain injury. The experimental  
123 procedures were approved by the local ethics committee (approval reference no. 3418, RCB  
124 no. 2016-A00715-46), and all procedures adhered to the Declaration of Helsinki.

125

### 126 2.2. Assessment of muscle activation

#### 127 2.2.1. *Experimental setup*

128 For *experiment I*, participants attended two identical testing sessions to assess the between-  
129 day reliability of the activation of the hamstring muscles (i.e., semitendinosus [ST],  
130 semimembranosus [SM], BFlh). Participants sat on an isokinetic dynamometer (Con-trex,  
131 CMV AG, Dübendorf, Switzerland) with non-compliant straps placed around the chest, the  
132 pelvis and the thigh. The hip and the knee were flexed at angles of  $90^\circ$  and  $45^\circ$ , respectively  
133 ( $0^\circ$  = neutral position for the hip and full extension for the knee). The  $45^\circ$  angle for the knee  
134 was chosen because it represents the angle at which the maximal knee flexion torque can be  
135 generated, i.e. the optimal angle (19). Visual feedback of the exerted torque signal was  
136 provided to the participant on a screen. The experimental setup used for *experiment II* was  
137 identical to that described above.

138

#### 139 2.2.2. *Mechanical data*

140 The torque signal from the isokinetic dynamometer was recorded and digitized by a USB data  
141 acquisition module (DT9804; Data Translation, Marlboro, MA, USA) at 1000 Hz. Torque  
142 was corrected for gravity and low-pass filtered at 20 Hz using a third-order Butterworth filter.

143

### 144 **2.2.3. Surface electromyography**

145 Myoelectric activity was recorded bilaterally with surface electrodes placed over the  
146 semitendinosus (ST), semimembranosus (SM) and biceps femoris (BF). Participants were  
147 seated on a customized piece of foam with a free space beneath each muscle to ensure that  
148 there was no contact between the electrodes and the seat. We used B-mode ultrasound  
149 (Aixplorer v11, Supersonic Imagine, Aix-en-Provence, France) to determine the appropriate  
150 placement for the ST, SM, and BF electrodes, longitudinally with respect to the muscle  
151 fascicle's alignment and away from the borders of the neighboring muscles. The superficial  
152 part of the BFsh is close to the popliteal fossa, so it was not possible to investigate this  
153 muscle. Therefore, we followed the SENIAM recommendation for electrode placement on the  
154 BF and considered the recorded myoelectrical activity originating from this pair of electrodes  
155 as being representative of both the short and the long heads (10). The skin was shaved and  
156 then cleaned with alcohol, and a pair of Ag/AgCl electrodes (Blue sensor N-00-S, Ambu,  
157 Copenhagen, Denmark) was attached to the skin with an inter-electrode distance of 20 mm  
158 (center-to-center). Raw EMG signals were pre-amplified 1000 times, band-pass filtered (10–  
159 500 Hz, third-order Butterworth filter) and sampled at 2000 Hz (Zerowire, Aurion, Milan,  
160 Italy). EMG and mechanical data were synchronized using a transistor–transistor logic pulse.

161

### 162 **2.2.4. Experimental tasks**

163 After a standardized warm-up (10 and 5 isometric contractions at 50% and 80% of maximal  
164 perceived intensity, respectively; 2 s hold and 2 s rest), participants performed three maximal



165 voluntary knee flexions. Each contraction was maintained for 3 to 5 s; contractions were  
166 separated by a 120-s rest period. The maximal value obtained from a moving average window  
167 of 300 ms was considered as the peak flexion torque. Using visual feedback, participants then  
168 performed three 10-s isometric knee flexions at 20% of MVC torque separated by 30 s of rest.  
169 *Experiment I* stopped at this point, but *experiment II* included a second part in which the time  
170 to exhaustion was measured. Specifically, after a 5-min rest period, participants performed an  
171 isometric knee flexion at 20% of MVC torque until task failure. They were strongly  
172 encouraged to maintain the torque as long as possible. Task failure was defined as the  
173 moment when the torque they produced decreased by more than 5% of the target level for at  
174 least 3 s. This task was performed with each leg, in a randomized order and separated by 5  
175 min of rest.

176

### 177 **2.2.5. Data processing**

178 All mechanical and EMG data were analyzed using MATLAB (R2017a, The Mathworks,  
179 Natick, MA, USA). To determine the maximal EMG amplitude, the Root Mean Square  
180 (RMS) of the EMG signal was calculated over a moving time window of 300 ms and the  
181 maximal value was considered as the maximal activation level. During the submaximal  
182 isometric knee flexions, the RMS EMG amplitude was calculated over 5 s at the time period  
183 corresponding to the lowest standard deviation of the torque signal. Then, this value was  
184 normalized to that measured during the MVC tasks. The ratio of activation between the  
185 hamstring muscles was calculated as the normalized RMS EMG of the considered muscle  
186 divided by the sum of normalized RMS EMG values of all three muscles.

187

## 188 **2.3. Estimation of torque-generating capacity**

### 189 **2.3.1. Magnetic resonance imaging (MRI)**

190 Both muscle volume and moment arm were estimated through Magnetic Resonance Imaging  
191 (MRI; 1.5 T, Intera Achieva, Philips, Amsterdam, Netherlands). Participants were first placed  
192 in supine position with their knees flexed at  $45^\circ$ , i.e., the same knee angle as that used for the  
193 experimental tasks. Flexible surface coils (SENSE, Philips, Amsterdam, Netherlands) were  
194 strapped to the medial and lateral sides of the knee. A volumetric sequence (3D T1 fast field  
195 echo, 5.17 min, FOV  $250\text{ mm} \times 179\text{ mm}$ , TR/TE = 24/11.5 ms, voxel size:  $1 \times 1 \times 2\text{ mm}$ , flip  
196 angle:  $50^\circ$ ) allowed an anatomical zone from half of the femur to half of the tibia to be  
197 imaged. This sequence was used to measure the moment arm. For each muscle, the knee  
198 flexion moment arm was defined as the shortest distance between the rotation center of the  
199 knee joint and the line of action of the considered muscle. To begin, the femoral condyle was  
200 segmented manually using 3D medical image processing software (Mimics, Materialise,  
201 Leuven, Belgium). The 3D coordinates of the lateral and medial femoral epicondyles were  
202 determined, and the center of the joint was calculated as the midpoint between these two  
203 points (5). Then, the distal part of the hamstring muscle-tendon unit (ST, SM, BF) was  
204 outlined (Fig. 1A). The centroid of the axial slices was calculated to reconstruct a line passing  
205 through, i.e. the musculotendon path. Finally, the perpendicular distance between the center  
206 of the joint and the musculotendon path was considered to be the moment arm. Due to their  
207 anatomical convergence, the distal tendon of the BFsh cannot be distinguished accurately  
208 from that of the BFlh (44). Consequently, we considered one common moment arm for both  
209 muscle heads, as has been done in other anatomical studies (37, 41).

210 A second acquisition sequence was dedicated to the measurement of the muscle volume. The  
211 participants were in a supine position, lying with their hips and knees fully extended. A spine  
212 coil (15 elements, SENSE, Philips) was placed under the pelvis and lower limbs to perform a  
213 volumetric sequence (3D T1 turbo fast field echo, 13.10 min, FOV  $360\text{ mm} \times 220\text{ mm}$ ,  
214 TR/TE = 14/6.9 ms, voxel size:  $0.8 \times 0.8 \times 2\text{ mm}$ , flip angle:  $20^\circ$ ). Slice thickness was 2 mm

215 without an inter-slice gap. Contiguous MR images were acquired from the iliac crest to half of  
216 the tibia to get images the hamstring heads (ST, SM, BF<sub>lh</sub> and BF<sub>sh</sub>), between their proximal  
217 and distal insertions. MR images of the ST, SM, BF<sub>lh</sub> and BF<sub>sh</sub> were segmented manually  
218 (Fig. 1B)

219

### 220 **2.3.2. B-mode ultrasound**

221 The field of view of the ultrasound transducer was too narrow (i.e., 42 mm) to image entire  
222 hamstring fascicles, which are typically longer than 12 cm for BF<sub>lh</sub> (44). To overcome this  
223 technical limitation, we used the built-in panoramic mode of the ultrasound device (Aixplorer  
224 V11, Supersonic Imagine). This mode uses an algorithm that fits a series of images, allowing  
225 the entire fascicles to be scanned within one continuous scan. The advantage of this approach  
226 over classical measurements from one B-mode image is that it does not require extrapolating  
227 the non-visible part of the fascicle (1). Participants were lying with the same hip and knee  
228 angles that were used during the submaximal task. The leg was attached to the dynamometer  
229 arm with a non-compliant strap. An ultrasound transducer (2–10 MHz, SL10-2, Supersonic  
230 Imagine, Aix-en-Provence, France) was placed over the muscle of interest and cross-sectional  
231 images were acquired in the longitudinal plane of the muscle to determine the path of the  
232 transducer. Scans began at the proximal insertion following the fascicle's plane in such a way  
233 that superficial and deep aponeuroses were visible. Scans progressed along the midline of the  
234 muscle until reaching the distal portion, at approximately at 90% of the femur length. The  
235 total scan time was 10 to 15 s. This was repeated for each muscle until two images with  
236 visible fascicles were obtained (Fig. 1C). A segmented line (with a spline fit) was used to  
237 model the fascicle and measure its length (ImageJ v1.48, National Institutes of Health,  
238 Bethesda, MD, USA). For the SM and BF<sub>lh</sub>, one fascicle was measured distally, medially,  
239 and proximally. The pennation angle was measured as the angle between the deep

240 aponeurosis and the fascicle. Then, the three values were averaged to get a representative  
241 value for the entire muscle. As the BFsh images were shorter, one or two fascicles were  
242 measured for each participant. The ST muscle is fusiform, and, therefore, its fascicle length  
243 was considered to be the distance between the distal and proximal insertions as determined  
244 using the MR images.

245

### 246 **2.3.3. Estimation of torque-generating capacity**

247 PCSA of SM, BF<sub>lh</sub> and BF<sub>sh</sub> was calculated as follows (22):

$$\text{PCSA} = \frac{\text{Muscle volume}}{\text{Fascicle length}} \times \cos(\text{Pennation angle})$$

248 where PCSA is expressed in cm<sup>2</sup>, muscle volume in cm<sup>3</sup>, and fascicle length in cm. Note that  
249 the fascicle length and pennation angle were assessed near the isometric optimal knee angle  
250 (45°; 0° = full extension of the knee). As ST muscle is fusiform, its PCSA was calculated as  
251 the ratio of the volume of the muscle to its length. For the head of each muscle, the product of  
252 PCSA with the moment arm (m) was considered as an index of torque-generating capacity.  
253 The ratio of torque-generating capacity between the hamstring muscles was calculated as the  
254 torque-generating capacity of the considered muscle divided by the sum of the torque-  
255 generating capacity of all three muscles.

256

### 257 **2.4. Estimation of an index of muscle torque**

258 During an isometric contraction, the difference of force produced by synergist muscles  
259 depends mainly on their PCSA, their activation, and their specific tension. Because hamstring  
260 muscles have similar fiber-types composition (9), and because the contractions were  
261 performed at low intensity during which it was likely that only slow fibers were recruited,  
262 specific tension was not expected to vary greatly between the muscle heads. Therefore, an  
263 index of muscle torque was calculated as follows:

264 Index of muscle torque = PCSA  $\times$  moment arm  $\times$  normalized RMS EMG  
265 where the index of muscle torque is expressed in arbitrary units (au), PCSA in cm<sup>2</sup>, moment  
266 arm in m and normalized RMS EMG in percentage of RMS EMG<sub>max</sub>. As was done for EMG  
267 and PCSA, we calculated the ratios of torque, i.e. BF/Hams, ST/Hams, and SM/Hams.

268

## 269 **2.5. Statistics**

270 Statistical analyses were performed using Statistica (v8, Statsoft, Tulsa, OK, USA).  
271 Distributions consistently passed the Kolmogorov–Smirnov normality test, and all data are  
272 reported as mean  $\pm$  SD. The intra-class correlation coefficient (ICC) and the typical error  
273 were calculated to determine the robustness of EMG data between the testing sessions. EMG  
274 amplitude were compared for muscles and legs using separate repeated-measures ANOVAs  
275 (within-subject factors: leg [dominant, non-dominant] and muscle [ST, SM, BF]). Fascicle  
276 length, pennation angle, muscle volume, moment arm and torque-generating capacity were  
277 compared for muscles and legs using separate repeated-measures ANOVAs (within-subject  
278 factors: leg [dominant, non-dominant] and muscle [ST, SM, BFsh, BFlh]). When the  
279 sphericity assumption was violated in repeated ANOVAs (Mauchly’s test), the Geisser–  
280 Greenhouse correction was used. When appropriate, post-hoc analyses were performed using  
281 Bonferroni tests.

282 To address the first aim (*experiment I*), the relationship between the distribution of activation  
283 and the distribution of torque-generating capacity among the heads of the hamstring was  
284 assessed using Pearson’s correlation coefficient. To address the second aim (*experiment I*), we  
285 compared each torque ratio (ST/Hams, SM/Hams, BF/Hams) for legs using a paired *t*-test.  
286 Also, we tested the correlation between sides using Pearson’s correlation coefficient. To  
287 address the third aim (*experiment II*), we first tested whether activation strategies changed  
288 during the sustained contraction by assessing the variability of the ratios of activation during

289 the fatiguing task using both the coefficient of variation and the typical error. The imbalance  
290 of the activation among the three muscle heads was assessed by calculating the standard  
291 deviation of their RMS EMG amplitude measured during the 10-s submaximal knee flexion  
292 tasks; i.e., the higher the standard deviation, the larger the activation difference between the  
293 muscles. The level of significance was set at  $P < 0.05$ . We report a correlation of 0.5 as large,  
294 0.3 as moderate, and 0.1 as small (7).

295

### 296 **3. RESULTS**

#### 297 **3.1. Experiment I**

298 The torque measured during the maximal isometric knee flexion tasks was significantly  
299 higher for the dominant leg than for the non-dominant leg. The values averaged between the  
300 two sessions were  $98.1 \pm 33.2$  Nm and  $88.5 \pm 29.4$  Nm ( $P < 0.001$ ).

301

##### 302 **3.1.1. *Muscle activation***

303 The between-day reliability of the normalized EMG amplitude measured during the  
304 submaximal isometric contraction at 20% MVC was fair to excellent (Table 1). ICC values  
305 ranged from 0.45 to 0.85 and the typical error ranged from 2.2% to 3.2% of RMS EMG<sub>max</sub>.  
306 Although the reliability was good for both legs, activation of the muscles in the dominant leg  
307 appeared to be slightly more reliable (Table 1). For the specific purpose of this article, we  
308 focused on the distribution of activation among the muscle heads by calculating the activation  
309 ratios, i.e. BF/Hams, ST/Hams, and SM/Hams. The inter-day reliability was good to excellent  
310 for all of these ratios except for the ST/Hams ratio for the non-dominant leg, which exhibited  
311 an ICC value slightly lower than 0.60 (Table 2). ICC values ranged from 0.57 to 0.88, and the  
312 typical error ranged from 2.7% to 5.6%. Considering this overall good reliability, EMG data  
313 were averaged between days for further analysis.

314 No differences in activation ratio were observed between legs ( $P = 0.34$ ,  $P = 0.83$ , and  $P =$   
315  $0.99$  for BF/Hams, SM/Hams, and ST/Hams, respectively). The similarity was further  
316 confirmed by the large correlation coefficients between legs ( $r = 0.75$  [ $P < 0.001$ ],  $0.55$  [ $P =$   
317  $0.008$ ], and  $0.68$  [ $P < 0.001$ ] for BF/Hams, SM/Hams, and ST/Hams, respectively). Notably,  
318 the activation ratios were highly variable between participants (Fig. 2A). For example, when  
319 considering the dominant leg, the ratio of activation ranged from 19.9 to 48.1% for BF/Hams,  
320 from 23.7 to 56.8% for SM/Hams and from 17.0 to 43.4% for ST/Hams.

321

### 322 **3.1.2. Torque-generating capacity**

323 Architectural characteristics of each head of the hamstring muscle and the associated statistics  
324 are presented in Table 3. For the sake of clarity, we only report the statistics associated with  
325 torque-generating capacity, which relates to the first aim of this study. There was no main  
326 effect of the leg ( $P = 0.73$ ) or the leg  $\times$  muscle interaction ( $P = 0.50$ ) on the torque-generating  
327 capacity. The absence of differences among the legs was further confirmed by the moderate to  
328 large correlation coefficients ( $r = 0.39$  [ $P = 0.07$ ],  $0.44$  [ $P = 0.038$ ], and  $0.72$  [ $P < 0.001$ ] for  
329 BF/Hams, SM/Hams, and ST/Hams, respectively). However, we observed a main effect of  
330 muscle ( $P < 0.001$ ). More precisely, the torque-generating capacity of ST was significantly  
331 lower than that of BF ( $-41.3 \pm 18.2\%$ ;  $P < 0.001$ ) and SM ( $-44.3 \pm 17.3\%$ ;  $P < 0.001$ ). As  
332 reported for the ratios of activation, a large variability between individuals was observed (Fig.  
333 2B). When considering the dominant leg, the ratio of torque-generating capacity ranged from  
334 30.0 to 46.9% for BF/Hams, from 32.9 to 50.6% for SM/Hams, and from 11.9 to 34.6% for  
335 ST/Hams.

336

### 337 **3.1.3. Relationship between activation and torque-generating capacity**

338 There was no significant correlation between the ratio of muscle activation and the ratio of  
339 torque-generating capacity, regardless of the muscle and the leg that were considered  
340 (dominant leg:  $r = 0.20$  [ $P = 0.36$ ],  $r = 0.03$  [ $P = 0.90$ ] and  $r = -0.31$  [ $P = 0.16$ ] for BF/Hams,  
341 SM/Hams and ST/Hams, respectively; non-dominant leg:  $r = 0.00$  [ $P = 0.99$ ],  $r = -0.02$  [ $P =$   
342  $0.91$ ] and  $r = -0.14$  [ $P = 0.54$ ] for BF/Hams, SM/Hams and ST/Hams, respectively). These  
343 results indicate that the imbalance of torque-generating capacity observed between the muscle  
344 heads was neither counteracted nor accentuated by activation. This contributed to an  
345 imbalance of the torque index, the magnitude of which varied greatly between participants.

346

#### 347 **3.1.4. Torque-sharing strategies**

348 When considering the torque index, which was calculated as the product of torque-generating  
349 capacity and the normalized EMG amplitude measured during the submaximal knee flexion,  
350 there was neither a main effect of the leg ( $P = 0.36$ ) nor the muscle  $\times$  leg interaction ( $P =$   
351  $0.51$ ). However, a main effect of muscle was found ( $P < 0.001$ ). Specifically, the torque index  
352 of ST ( $7.0 \pm 2.8$  [au]) was lower than that of BF ( $13.7 \pm 6.4$ ;  $P < 0.001$ ) and SM ( $16.1 \pm 6.1$ ;  $P$   
353  $< 0.001$ ). There were no significant differences between BF and SM ( $P = 0.19$ ). When  
354 considering the dominant leg, the torque index ratio reached  $18.5 \pm 6.8\%$  for ST/Hams,  $37.7 \pm$   
355  $10.1\%$  for BF/Hams, and  $43.8 \pm 9.9\%$  for SM/Hams (Fig. 3A). There was a significant  
356 correlation between the torque index ratios of the dominant and non-dominant legs for  
357 ST/Hams ( $r = 0.63$  [ $P = 0.002$ ]), BF/Hams ( $r = 0.60$  [ $P = 0.003$ ]) and SM/Hams ( $r = 0.48$  [ $P$   
358  $= 0.025$ ]) (Fig. 3B). The group distribution of the torque index ratios displayed in Fig. 3  
359 reveals a large inter-individual variability.

360

## 361 **3.2. Experiment II**



362 When considering the dominant leg, the coefficient of variation of the activation ratios  
363 measured during the limit time to exhaustion was low, i.e., 9.4% for ST/Hams, 9.5% for  
364 SM/Hams, and 11.4% for BF/Hams. The typical error (TE) was 5.7% for ST/Hams, 4.5% for  
365 SM/Hams, and 5.1% for BF/Hams. Similar values were reported for the non-dominant leg  
366 (CV: 7.4%, 10.6%, and 12.8%; TE: 2.9%, 6.3%, and 6.9% for ST/Hams, SM/Hams and  
367 BF/Hams, respectively). Therefore, we concluded that the activation strategies did not change  
368 drastically during the sustained submaximal contraction. The mean standard deviation of the  
369 RMS EMG amplitude measured during the 10-s contractions that preceded the sustained  
370 contraction was  $3.2 \pm 1.9\%$  of RMS EMG<sub>max</sub> (range: 0.4–8.3%) and  $3.1 \pm 1.6\%$  of RMS  
371 EMG<sub>max</sub> (range: 0.6–7.2%) for the dominant and non-dominant legs, respectively. Participants  
372 maintained the targeted torque for  $466 \pm 190$  s (range: 195–1037 s) with their dominant legs  
373 and for  $473 \pm 210$  s (range: 163–1260 s) with their non-dominant legs. There was a significant  
374 negative correlation between the standard deviation values and the time to exhaustion ( $r = -$   
375  $0.52$  [ $P < 0.001$ ] and  $r = -0.42$  [ $P = 0.011$ ] for the dominant and non-dominant legs,  
376 respectively) (Fig. 4). These correlations indicate that the larger the activation difference  
377 between the muscle heads, the shorter the time to exhaustion.

## 378 4. DISCUSSION

379 Three novel findings resulted from this study. First, there was no correlation between the  
380 distribution of activation between the heads of the hamstring and the distribution of torque-  
381 generating capacity. Secondly, the torque-sharing strategy varied greatly between participants  
382 but it was similar for the participants' two legs. Thirdly, the larger the imbalance of activation  
383 across the muscle heads, the lower the muscle endurance. These results provide a deeper  
384 understanding of the interplay between the activation a muscle receives and its mechanical  
385 characteristics. By demonstrating a relationship between activation strategies and endurance  
386 performance, our findings also provide the foundation for future work to explore the roles of  
387 different muscle coordination strategies in motor performance. These results may have  
388 clinical relevance as they provide a basis for considering muscle coordination strategies as an  
389 intrinsic risk factor for hamstring strain injury.

390

### 391 4.1. Individual muscle activation strategies

392 When the entire sample of participants was considered, the activation ratios were similar for  
393 different muscles, which might lead to the conclusion that the activation is shared roughly  
394 equally among the three heads. However, inspection of the data for individual participants  
395 revealed a large variability, as illustrated by the SM/Hams ratio, which ranged from 23.7% to  
396 56.8% (Fig. 2A). Large individual differences in EMG amplitude ratio already have been  
397 reported for knee extensors (14) and ankle plantar flexors (21). For example, Hug et al. (14)  
398 reported a VL/VM activation ratio ranging from 33.6 to 74.7% during an isometric knee  
399 extension task performed at 20% of MVC, with an almost equal number of participants  
400 demonstrating either greater VL activation or greater VM activation. Overall, these results  
401 highlight how group data may lead researchers/clinicians to underestimate important

402 differences between individuals, potentially resulting in the incorrect conclusion that  
403 individuals use similar activation strategies.

404 Importantly, the aforementioned differences between individuals in muscle activation can  
405 only be considered as evidence of individual-specific strategies if these strategies persist over  
406 time (11). Our findings showed an overall good between-day reliability of muscle activation  
407 ratios, which was reflective of robust activation strategies. In addition, the vast majority of  
408 studies have reported EMG values from one leg under the basic assumption that muscle  
409 activations are similar for both legs. Ounpuu & Winter (29) did not confirm this hypothesis  
410 for multiple muscles during gait and concluded that pooled subject data may conceal bilateral  
411 differences. In contrast, during a submaximal isometric contraction with fewer degrees of  
412 freedom, we observed large significant correlations of the activation ratios between legs ( $0.55$   
413  $< r < 0.75$ ). Although these correlations do not mean that activation strategies are strictly the  
414 same, they confirm that these strategies are consistent between legs, which further supports  
415 the hypothesized existence of individual muscle coordination signatures (15). Importantly, the  
416 functional consequences of such individual differences in activation strategy require that the  
417 muscle torque-generating capacity and its interplay with activation be taken into account.

418

#### 419 **4.2. Muscle torque-generating capacity and its relationship with activation**

420 To date, hamstring PCSA has been measured mainly in cadavers because of technical  
421 limitations related to the measurement of muscle fascicle length *in vivo*, especially for  
422 muscles with complex fiber arrangement such as the hamstrings (18, 42, 44). Taking  
423 advantage of panoramic ultrasound, we estimated the distribution of PCSA and reported large  
424 differences between muscles; the PCSA of BF and SM was similar, while that of ST was  
425 consistently smaller (Table 3). Our values concur with those reported from cadavers (12.1%,  
426 46.5% and 41.4% for ST/Hams, SM/Hams, BF/Hams, respectively (42)). These differences in

427 force-generating capacity can be either compensated or exacerbated at the joint level by  
428 different moment arms. Although ST exhibited a longer moment arm ( $5.7 \pm 0.7$  cm) than SM  
429 ( $4.8 \pm 0.5$  cm) and BF ( $4.6 \pm 0.4$  cm), the longer moment arm did not completely compensate  
430 for its lower torque-generating capacity. Our results highlighted a large variability in torque  
431 and force-generating capacity between muscle heads. Importantly, the magnitude of these  
432 differences varies greatly between participants.

433 Previous studies have shown that the activation a muscle receives and its mechanical  
434 properties are coupled (12, 14). For instance, Hug et al. (14) showed that the greater the  
435 PCSA of VL compared with VM, the stronger the bias of the activation toward VL.  
436 Inevitably, this induces a large imbalance of force between the synergist muscles crossing the  
437 same joint. In this study, we observed neither positive nor negative correlations between the  
438 PCSA and the EMG ratio or between the torque-generating capacity and the EMG ratio. Why  
439 our results are different from previous results (14) is unclear. It might be explained by  
440 different functional roles of the muscles crossing the knee joint, with the vastii mainly  
441 generating torque and the hamstring mainly controlling the direction of the torque (40). It is  
442 also possible that the functional consequences of such a coupling would have negative  
443 consequences for the non-muscular structures that surround the hamstring muscles. Indeed,  
444 the difference in force-generating capacity between VL and VM (for which a coupling was  
445 observed) is less than what we observed herein between the heads of the hamstring. As such,  
446 a positive correlation between torque-generating capacity and activation of the hamstring  
447 would have induced a much larger imbalance of torque than that observed for the *vastii*.  
448 However, it is important to note that, even though this positive correlation was not observed,  
449 neither was a negative correlation observed, meaning that the differences in torque-generating  
450 capacity were not counterbalanced by opposite differences in activation. This has led to a  
451 wide range of individual torque-sharing strategies.

452

### 453 **4.3. Individual-specific torque-sharing strategies**

454 The muscle heads displayed differences in torque contribution, e.g., BF/Hams, SM/Hams and  
455 ST/Hams accounted for  $37.9 \pm 10.1\%$  (range: 20.2–54.8%),  $43.9 \pm 9.8\%$  (range: 28.3–63.7%)  
456 and  $18.3 \pm 6.7\%$  (range: 9.1–39.9%) of the torque-generating capacity, respectively (Fig. 3A).  
457 Interestingly, comparable ratios of force (without considering the moment arm) were  
458 estimated by a musculoskeletal model during the stance phase of high speed running (6).  
459 Beyond the between-muscle differences, we believe that the description of the individual-  
460 specific torque-sharing strategies is the main result of this study (Fig. 3A). For example, the  
461 torque produced by BF and ST in participant #1 accounted for 54.8% and 16.8% of the total  
462 torque required to reach the target of 20% of the MVC torque. To complete the same task,  
463 participant #23 generated 24.2% of the total torque with BF and 39.9% with ST. These  
464 individual differences resulted from interindividual variability of the distribution of both  
465 activation and torque-generating capacity. Even though interindividual variability of muscle  
466 activation is logically larger at relatively low contraction intensities (14), as studied here, the  
467 absolute between-muscle differences in torque would be greater at higher intensities, despite a  
468 more balanced activation.

469 The interindividual variability of muscle coordination strategies may support the idea that  
470 individuals can perform the task with a range of *good-enough strategies* (23), rather than  
471 requiring an iterative optimization to a specific strategy. In short, following a trial-and-error  
472 process, nervous system saves successful programs that can be recalled when facing a similar  
473 task (23). Thus, the contraction history may influence both the number of motor programs  
474 available to complete the task and the efficiency of those programs (32). Such individual  
475 differences might have functional consequences for the musculoskeletal system (15) and  
476 might affect motor performance (34, 35).

477

#### 478 **4.4. Distribution of muscle activation influences muscle performance**

479 The observed individual differences in the distribution of muscle activation might have  
480 important functional consequences with some strategies being less effective. For example, if  
481 one muscle is activated to a greater extent than required by the task, which is inevitably the  
482 case when activation among the synergists is imbalanced, its metabolic demand would be  
483 higher and, therefore, fatigue would develop sooner (39). Fatigue models predict that the task  
484 is interrupted, or force is decreased, to prevent physiological failure (26, 28). Therefore, it is  
485 possible that the first muscle that reaches this “threshold” would limit the overall  
486 performance. In this way, Prilutsky and Zatsiorsky (31) suggested that fatigue may be  
487 minimized if stress is more evenly distributed among muscles. Our results support the  
488 aforementioned hypothesis. To begin, although it is difficult to interpret the change in EMG  
489 amplitude as a change in activation during a fatiguing task (8, 13), the ratios of EMG  
490 amplitudes did not vary during the fatiguing task, allowing us to assume that the activation  
491 strategies persisted throughout the task. It was important to test this (albeit indirectly),  
492 because a change in activation strategy with fatigue had already been reported in some studies  
493 (2, 17), but not in others (33). Second, we estimated the imbalance of activation among the  
494 muscle heads by calculating the standard deviation of the EMG amplitude. Note that we  
495 found a positive correlation between the magnitude of the standard deviation and the highest  
496 EMG amplitude value among muscle heads ( $r = 0.50$  [ $P = 0.002$ ] and  $r = 0.60$  [ $P < 0.001$ ] for  
497 the dominant leg and the non-dominant leg, respectively). This confirmed our assumption that  
498 the more imbalanced the activation between the muscle heads, the higher the activation of the  
499 most activated muscle. Third, and more importantly, we observed a strong (dominant leg) or  
500 moderate (non-dominant leg) negative correlation between the standard deviation values and  
501 the time to exhaustion (Fig. 4). This indicates that the larger the difference in activation

502 between the muscle heads, the shorter the time to exhaustion. Although the finding that  
503 muscle activation strategies influence endurance performance is novel, one should keep in  
504 mind that other factors, such as muscle architecture (3), muscle typology and training level  
505 (4), are known to affect endurance performance. This multifactorial origin of endurance  
506 performance may explain why the coefficients of correlation are not higher. Even so, we  
507 believe that our results support the concept that individual coordination strategies may have  
508 functional consequences, such as an effect on motor performance. To the best of our  
509 knowledge, this is a novel finding. It has potential importance for hamstring strain injuries,  
510 which have been argued to be related to fatigability and the associated compensation between  
511 synergists (34, 35).

512

#### 513 **4.5. Methodological considerations**

514 Some methodological considerations should be kept in mind when interpreting the present  
515 data. First, we used surface EMG amplitude as a surrogate for muscle activation. Therefore, it  
516 is important to consider the factors that could influence the relationship between EMG  
517 amplitude and muscle activation. Among these factors, we believe that crosstalk and the  
518 normalization procedure are the most important. Although EMG signals from the hamstring  
519 might be affected by crosstalk, we systematically used B-mode ultrasound to place the  
520 electrodes over the muscle of interest, away from the borders where signal contamination is  
521 strongest. This procedure allowed us to distinguish between the SM and ST muscles, which  
522 are difficult to differentiate using palpation (10). It is important to note that if we run the same  
523 analysis considering only the medial (MH, i.e. SM + ST) and lateral hamstrings (LH, i.e. BF),  
524 there is still no correlation between LH/(LH+MH) activation ratio and LH/(LH+MH) torque-  
525 generating capacity ratio. Taken together with the consistency of the EMG data between days  
526 and between legs, we are confident that crosstalk did not interfere with our main conclusions.

527 Also, the accuracy of between-muscle and between-participant comparisons lies in the truly  
528 maximal voluntary activation during the maximal contraction used to normalize EMG  
529 amplitude. Using the twitch interpolation method (38), previous studies have reported that  
530 young healthy participants (similar to those in our experiment) are able to achieve near-  
531 complete activation of their hamstrings ( $97.1 \pm 2.2\%$  (24) and  $98.7 \pm 1.3\%$  (20)). Therefore,  
532 the EMG amplitude measured during maximal contractions likely represents the true maximal  
533 muscle activation.

534 Second, we estimated muscle torque-generating capacity from PCSA and the moment arm  
535 measured at rest. Even though fascicles shorten during contraction, therefore affecting PCSA  
536 (27), previous works demonstrated that PCSA measured at rest is as strongly related with  
537 muscle strength as PCSA measured during MVC (25). It is also possible that muscle  
538 contraction induced slight changes in both the line of action and the joint center of rotation,  
539 leading to modification of muscle moment arm. To the best of our knowledge, such changes  
540 have not been reported. Although it is possible that such alterations may occur, their  
541 magnitude would have remained low during such a low intensity isometric contraction, i.e.  
542 20% MVC.

543 Finally, although we considered two important mechanical factors (i.e., PCSA and moment  
544 arm) that influence the torque-generating capacity during such an isometric task, we did not  
545 consider either the specific tension or the individual muscle force-length relationship.  
546 However, to date, no experimental technique is available to measure these mechanical factors  
547 accurately. In addition, specific tension varies only marginally between muscles with similar  
548 fiber type composition (30, 43), especially at low contraction intensities during which slow  
549 fibers are recruited preferentially. Therefore, we believe that considering specific tension  
550 would not have affected the between-muscle differences in torque production. In addition,  
551 estimating the between-muscles differences in torque-generating capacity during an isometric



552 task should take into account possible between-muscles differences in the shape of the force–  
553 length relationship. Although such a relationship cannot be determined for each individual  
554 muscle head, the fascicle lengths we measured near the optimal angle were similar to the  
555 optimal length previously reported from cadaver preparations (e.g.  $10.7 \pm 1.4$  cm vs.  $11.0 \pm$   
556  $2.1$  cm for BFsh in Ward (42)). Therefore, it is reasonable to consider that each of the three  
557 heads did operated at a similar relative length.

558

## 559 **5. CONCLUSIONS**

560 Both the distribution of activation and the distribution of torque-generating capacity varied  
561 greatly between individuals. In the absence of a negative coupling between activation and  
562 torque-generating capacity, a wide range of torque-sharing strategies was observed. To the  
563 best of our knowledge, this is the first study to show a relationship between individual-  
564 specific activation strategies and performance during an endurance task. Overall, this study  
565 provides new insight into the coordination between the heads of the hamstring during  
566 submaximal contractions. The observed variability between individuals provide a basis from  
567 which to consider muscle coordination strategies as an intrinsic risk factor for hamstring  
568 strain injury.

569

570 **ACKNOWLEDGMENTS:**

571 The authors thank the technicians from the lab Imagerie par Résonance Magnétique Médicale  
572 et Multi-modalités (IR4M-UMR8081), for their assistance with MRI data collection.

573

574 **GRANTS:**

575 S. Avrillon was supported by a scholarship funded by the French Ministry of Research. F.

576 Hug was supported by a fellowship from the Institut Universitaire de France (IUF).

577

578 **DISCLOSURES:**

579 No conflicts of interest, financial or otherwise, are declared by the authors. Authors declare  
580 that they have no conflicts of interest relevant to the content of this original research article.

581 TABLES:

582

583 Table 1. RMS EMG amplitude of the biceps femoris (BF) semimembranosus (SM) and  
 584 semitendinosus (ST) muscles during the submaximal isometric knee extension task. ICC,  
 585 intra-class coefficient correlation; TE, typical error. Values are means  $\pm$  SD.

586

	DOMINANT LEG			NON-DOMINANT LEG			MAIN EFFECT		
	BF (% max)	SM (% max)	ST (% max)	BF (% max)	SM (% max)	ST (% max)	Leg	Muscle	Interaction
<b>DAY 1</b>	13.0 $\pm$ 4.4	14.6 $\pm$ 4.7	11.8 $\pm$ 5.4	12.7 $\pm$ 3.3	14.1 $\pm$ 4.1	12.2 $\pm$ 3.6			
<b>DAY 2</b>	13.2 $\pm$ 4.8	15.0 $\pm$ 4.8	12.8 $\pm$ 5.5	11.8 $\pm$ 3.8	14.6 $\pm$ 4.7	11.4 $\pm$ 5.3			
<b>AVERAGE</b>	13.1 $\pm$ 4.3	14.8 $\pm$ 4.4 <sup>a</sup>	12.3 $\pm$ 5.2 <sup>b</sup>	12.2 $\pm$ 3.0	14.3 $\pm$ 3.9 <sup>a</sup>	11.8 $\pm$ 3.9 <sup>b</sup>	P = 0.34	<b>P = 0.036</b>	P = 0.83
<b>ICC</b>	0.74	0.74	0.85	0.45	0.59	0.51			
<b>TE</b>	2.4	2.5	2.2	2.7	2.9	3.2			

587 Superscript letters denote significant differences with: <sup>a</sup>ST, <sup>b</sup>SM.

588

589 Table 2. Activation ratios between the heads of the hamstring muscle group. ICC, intra-class  
 590 coefficient correlation; TE, typical error. Values are means  $\pm$  SD.

591

	DOMINANT LEG			NON-DOMINANT LEG		
	BF/Hams (%)	SM/Hams (%)	ST/Hams (%)	BF/Hams (%)	SM/Hams (%)	ST/Hams (%)
<b>Day 1</b>	33.4 $\pm$ 8.0	37.3 $\pm$ 7.8	29.3 $\pm$ 7.4	32.6 $\pm$ 7.7	36.2 $\pm$ 8.7	31.1 $\pm$ 7.0
<b>Day 2</b>	32.7 $\pm$ 8.6	36.8 $\pm$ 7.4	30.5 $\pm$ 7.6	31.9 $\pm$ 9.2	38.8 $\pm$ 8.2	29.3 $\pm$ 9.6
<b>ICC</b>	0.77	0.88	0.68	0.72	0.75	0.57
<b>TE</b>	4.1	2.7	4.4	4.6	4.4	5.6

592

593

594 Table 3. Morphological and architectural data for the biceps femoris long head (BF<sub>lh</sub>), short  
 595 head (BF<sub>sh</sub>), semimembranosus (SM) and semitendinosus (ST) muscles. fl,

596 fascicle length; PA, pennation angle; PCSA, physiological cross-sectional area; TGC, torque-  
 597 generating capacity. Values are means  $\pm$  SD.

598

	DOMINANT LEG				NON-DOMINANT LEG				MAIN EFFECT		
	BFsh	BFlh	SM	ST	BFsh	BFlh	SM	ST	Leg	Muscle	Interaction
<b>VOLUME</b>	86.3 $\pm$	184.6 $\pm$	207.5 $\pm$	173.4 $\pm$	85.2 $\pm$	178.2 $\pm$ 47.6 <sup>c</sup>	207.7 $\pm$	178.0 $\pm$	P =	<b>P &lt;</b>	P = 0.24
<b>(CM<sup>3</sup>)</b>	37.6 <sup>bcd</sup>	41.6 <sup>ac</sup>	56.7 <sup>abd</sup>	67.3 <sup>ac</sup>	34.7 <sup>bcd</sup>		53.7 <sup>abd</sup>	67.5 <sup>c</sup>	0.71	<b>0.001</b>	
<b>FL (CM)</b>	10.7 $\pm$	12.1 $\pm$	8.9 $\pm$	17.2 $\pm$	10.8 $\pm$	11.9 $\pm$ 1.6 <sup>d</sup>	9.0 $\pm$	17.1 $\pm$	P =	<b>P &lt;</b>	P = 0.86
	1.4 <sup>d</sup>	1.7 <sup>cd</sup>	1.4 <sup>bd</sup>	4.4 <sup>abc</sup>	1.2 <sup>d</sup>		1.2 <sup>bd</sup>	3.9 <sup>abc</sup>	0.80	<b>0.001</b>	
<b>PA (°)</b>	12.4 $\pm$	9.0 $\pm$	10.7 $\pm$		11.9 $\pm$	9.3 $\pm$ 1.9 <sup>ac</sup>	11.1 $\pm$		P =	<b>P &lt;</b>	P = 0.42
	2.4 <sup>bc</sup>	1.6 <sup>ac</sup>	2.0 <sup>ab</sup>		2.8 <sup>bc</sup>		1.8 <sup>ab</sup>		0.89	<b>0.001</b>	
<b>PCSA (CM<sup>2</sup>)</b>	7.9 $\pm$	15.2 $\pm$	23.4 $\pm$	10.2 $\pm$	7.8 $\pm$	15.0 $\pm$ 4.1 <sup>acd</sup>	22.9 $\pm$	10.7 $\pm$	P =	<b>P &lt;</b>	P = 0.69
	3.3 <sup>bcd</sup>	3.6 <sup>acd</sup>	7.6 <sup>abd</sup>	3.9 <sup>abc</sup>	3.1 <sup>bcd</sup>		6.0 <sup>abd</sup>	3.8 <sup>abc</sup>	0.74	<b>0.001</b>	
<b>MOMENT</b>			4.8 $\pm$	5.7 $\pm$			4.8 $\pm$	5.8 $\pm$	P =	<b>P &lt;</b>	P = 0.19
<b>ARM (CM)</b>	4.6 $\pm$ 0.4 <sup>bc</sup>		0.5 <sup>ac</sup>	0.7 <sup>ab</sup>		4.5 $\pm$ 0.4 <sup>bc</sup>	0.4 <sup>ac</sup>	0.6 <sup>ab</sup>	0.36	<b>0.001</b>	
<b>TGC</b>	107.3 $\pm$ 34.8 <sup>c</sup>		113.3 $\pm$	60.2 $\pm$		104.5 $\pm$ 34.1 <sup>c</sup>	110.1 $\pm$	63.2 $\pm$	P =	<b>P &lt;</b>	P = 0.50
			44.7 <sup>c</sup>	27.9 <sup>ab</sup>			33.0 <sup>c</sup>	26.3 <sup>ab</sup>	0.73	<b>0.001</b>	

599 Letters in superscript denotes significant differences with: <sup>a</sup>BFsh, <sup>b</sup>BFlh, <sup>c</sup>SM, <sup>d</sup>ST.

600 FIGURE CAPTIONS:

601

602 Fig. 1. Individual example of estimating the torque-generating capacity from MRI and  
603 ultrasound images. A. Muscle volume reconstruction of semitendinosus (ST),  
604 semimembranosus (SM) biceps femoris long head (BF<sub>lh</sub>) and short head (BF<sub>sh</sub>). B.  
605 Reconstruction of musculotendon path after manual segmentation to measure the moment arm  
606 (i.e., the shortest distance between the joint center and the musculotendon path). C. Panoramic  
607 US image of SM to determine fascicle length. Muscle fascicles were imaged through a  
608 longitudinal scan performed in the fascicle's plane. Particular care was taken to measure fully  
609 visible fascicles in a region of interest including clear aponeuroses.

610

611 Fig. 2. Box charts depicting mean values (line)  $\pm$  one standard deviation (box) and individual  
612 values (scatters) of EMG amplitude (A) and torque-generating capacity (B). EMG amplitude  
613 referred to normalized EMG RMS values. Group distribution is given for the ratio of muscle  
614 activation (A) and the ratio of torque-generating capacity (B).

615

616 Fig. 3. (A) Group distribution of the torque index ratio. The correlations for BF, SM and ST  
617 (B) indicate that torque-sharing strategies are similar between legs. The solid line represents  
618 equal torque generation between legs.

619

620 Fig. 4. Correlations between the imbalance of muscle activation and the time to task failure.  
621 The imbalance of activation was assessed through the standard deviation of normalized RMS  
622 EMG across the muscle heads. These correlations indicate that the larger the imbalance in  
623 muscle activation among synergists, the sooner failure occurs in the endurance task. Note that

624 the coefficient of correlation was even higher when the two participants who exhibited the  
625 longest times to exhaustion are not considered.

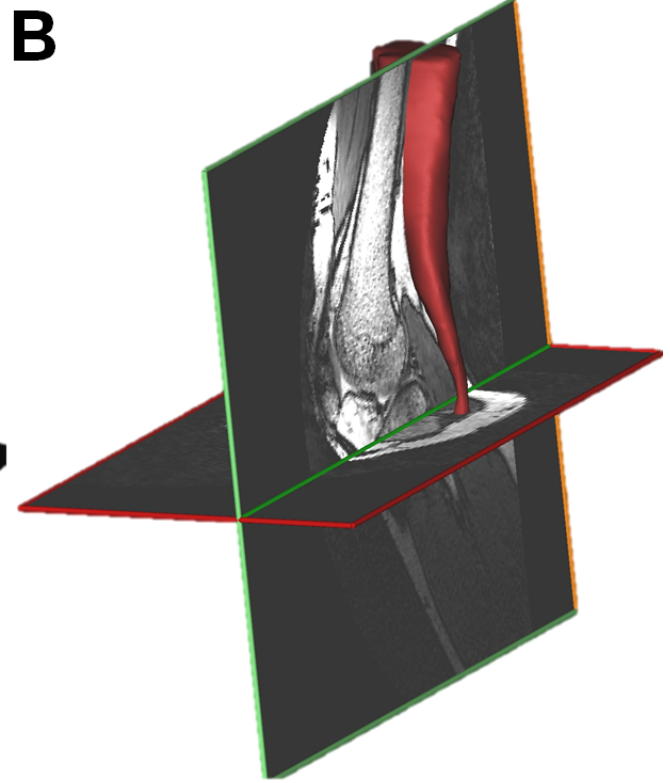
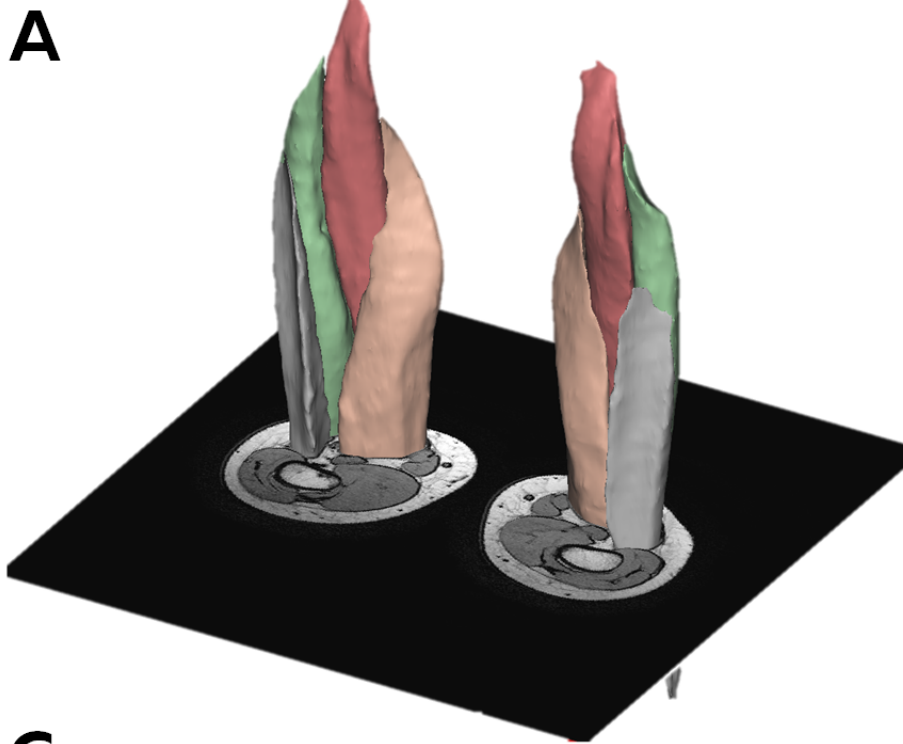
626

- 628 1. **Adkins AN, Franks PW, and Murray WM.** Demonstration of extended field-of-  
629 view ultrasound's potential to increase the pool of muscles for which in vivo fascicle length is  
630 measurable. *J Biomech* 2017.
- 631 2. **Akima H, Foley JM, Prior BM, Dudley GA, and Meyer RA.** Vastus lateralis  
632 fatigue alters recruitment of musculus quadriceps femoris in humans. *J Appl Physiol (1985)*  
633 92: 679-684, 2002.
- 634 3. **Biewener AA.** Locomotion as an emergent property of muscle contractile dynamics. *J*  
635 *Exp Biol* 219: 285-294, 2016.
- 636 4. **Cairns SP, Knicker AJ, Thompson MW, and Sjogaard G.** Evaluation of models  
637 used to study neuromuscular fatigue. *Exerc Sport Sci Rev* 33: 9-16, 2005.
- 638 5. **Cappozzo A, Catani F, Della Croce U, and Leardini A.** Position and orientation in  
639 space of bones during movement: anatomical frame definition and determination. *Clin*  
640 *Biomech* 10: 171-178, 1995.
- 641 6. **Chumanov ES, Heiderscheit BC, and Thelen DG.** Hamstring musculotendon  
642 dynamics during stance and swing phases of high-speed running. *Med Sci Sports Exerc* 43:  
643 525-532, 2011.
- 644 7. **Cohen J.** Differences between Correlation Coefficients. In: *Statistical Power Analysis*  
645 *for the Behavioral Sciences (Revised Edition)* Academic Press, 1977, p. 109-143.
- 646 8. **Farina D, Merletti R, and Stegeman DF.** Biophysics of the Generation of EMG  
647 Signals. In: *Electromyography* John Wiley & Sons, Inc., 2005, p. 81-105.
- 648 9. **Garrett WE, Jr., Califf JC, and Bassett FH, 3rd.** Histochemical correlates of  
649 hamstring injuries. *Am J Sports Med* 12: 98-103, 1984.
- 650 10. **Hermens HJ, Freriks K, Disselhorst-Klug C, and Rau G.** Development of  
651 recommendations for SEMG sensors and sensor placement procedures. *J Electromyogr*  
652 *Kinesiol* 2000.
- 653 11. **Horst F, Mildner M, and Schollhorn WI.** One-year persistence of individual gait  
654 patterns identified in a follow-up study - A call for individualised diagnose and therapy. *Gait*  
655 *Posture* 58: 476-480, 2017.
- 656 12. **Hudson AL, Taylor JL, Gandevia SC, and Butler JE.** Coupling between  
657 mechanical and neural behaviour in the human first dorsal interosseous muscle. *J Physiol* 587:  
658 917-925, 2009.
- 659 13. **Hug F.** Can muscle coordination be precisely studied by surface electromyography? *J*  
660 *Electromyogr Kinesiol* 21: 1-12, 2011.
- 661 14. **Hug F, Goupille C, Baum D, Raiteri BJ, Hodges PW, and Tucker K.** Nature of the  
662 coupling between neural drive and force-generating capacity in the human quadriceps muscle.  
663 *Proc Biol Sci* 282: 2015.
- 664 15. **Hug F, and Tucker K.** Muscle Coordination and the Development of  
665 Musculoskeletal Disorders. *Exerc Sport Sci Rev* 2017.
- 666 16. **Hunter SK, Duchateau J, and Enoka RM.** Muscle Fatigue and the Mechanisms of  
667 Task Failure. *Med Sci Sports Exerc* 2004.
- 668 17. **Hunter SK, and Enoka RM.** Changes in muscle activation can prolong the  
669 endurance time of a submaximal isometric contraction in humans. *J Appl Physiol (1985)* 94:  
670 108-118, 2003.
- 671 18. **Kellis E, Galanis N, Natsis K, and Kapetanios G.** Muscle architecture variations  
672 along the human semitendinosus and biceps femoris (long head) length. *J Electromyogr*  
673 *Kinesiol* 20: 1237-1243, 2010.

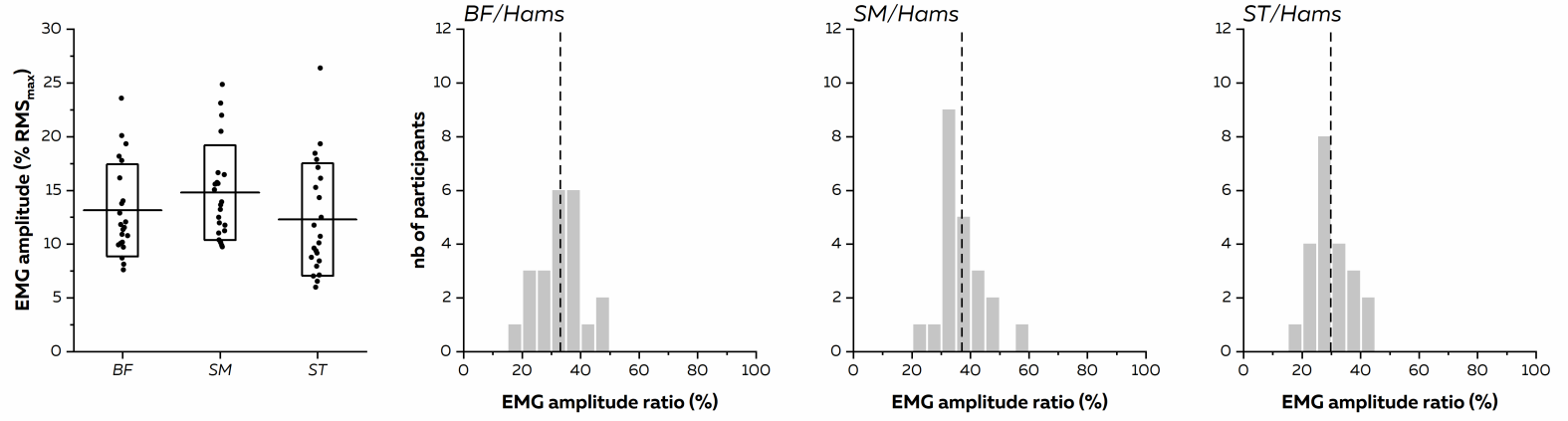
- 674 19. **Kilgallon M, Donnelly AE, and Shafat A.** Progressive resistance training  
675 temporarily alters hamstring torque-angle relationship. *Scan J Med Sci Sports* 17: 18-24,  
676 2007.
- 677 20. **Kirk EA, and Rice CL.** Contractile function and motor unit firing rates of the human  
678 hamstrings. *J Neurophysiol* 117: 243-250, 2017.
- 679 21. **Lacourpaille L, Nordez A, and Hug F.** The nervous system does not compensate for  
680 an acute change in the balance of passive force between synergist muscles. *J Exp Biol* 2017.
- 681 22. **Lieber RL, and Ward SR.** Skeletal muscle design to meet functional demands.  
682 *Philos Trans R Soc Lond B Biol Sci* 366: 1466-1476, 2011.
- 683 23. **Loeb GE.** Optimal isn't good enough. *Biol Cybern* 106: 757-765, 2012.
- 684 24. **Marshall PW, Lovell R, Jeppesen GK, Andersen K, and Siegler JC.** Hamstring  
685 muscle fatigue and central motor output during a simulated soccer match. *PLoS One* 9:  
686 e102753, 2014.
- 687 25. **Massey G, Evangelidis P, and Folland J.** Influence of contractile force on the  
688 architecture and morphology of the quadriceps femoris. *Exp Physiol* 100: 1342-1351, 2015.
- 689 26. **Millet GY.** Can neuromuscular fatigue explain running strategies and performance in  
690 ultra-marathons?: the flush model. *Sports Med* 41: 489-506, 2011.
- 691 27. **Narici MV, Binzoni T, Hiltbrand E, Fasel J, Terrier F, and Cerretelli P.** In vivo  
692 human gastrocnemius architecture with changing joint angle at rest and during graded  
693 isometric contraction. *J Physiol* 496 ( Pt 1): 287-297, 1996.
- 694 28. **Noakes TD, and St Clair Gibson A.** Logical limitations to the "catastrophe" models  
695 of fatigue during exercise in humans. *Br J Sports Med* 38: 648-649, 2004.
- 696 29. **Ounpuu S, and Winter DA.** Bilateral electromyographical analysis of the lower  
697 limbs during walking in normal adults. *Electroencephalogr Clin Neurophysiol* 72: 429-438,  
698 1989.
- 699 30. **Powell PL, Roy RR, Kanim P, Bello MA, and Edgerton VR.** Predictability of  
700 skeletal muscle tension from architectural determinations in guinea pig hindlimbs. *J Appl*  
701 *Physiol Respir Environ Exerc Physiol.* 57: 1715-1721, 1984.
- 702 31. **Prilutsky BI, and Zatsiorsky VM.** Optimization-based models of muscle  
703 coordination. *Exerc Sport Sci Rev* 30: 32-38, 2002.
- 704 32. **Ranganathan R, Wieser J, Mosier KM, Mussa-Ivaldi FA, and Scheidt RA.**  
705 Learning redundant motor tasks with and without overlapping dimensions: facilitation and  
706 interference effects. *J Neurosci* 34: 8289-8299, 2014.
- 707 33. **Rudroff T, Christou EA, Poston B, Bojsen-Moller J, and Enoka RM.** Time to  
708 failure of a sustained contraction is predicted by target torque and initial electromyographic  
709 bursts in elbow flexor muscles. *Muscle Nerve* 35: 657-666, 2007.
- 710 34. **Schuermans J, Van Tiggelen D, Danneels L, and Witvrouw E.** Biceps femoris and  
711 semitendinosus--teammates or competitors? New insights into hamstring injury mechanisms  
712 in male football players: a muscle functional MRI study. *Br J Sports Med* 48: 1599-1606,  
713 2014.
- 714 35. **Schuermans J, Van Tiggelen D, Danneels L, and Witvrouw E.** Susceptibility to  
715 Hamstring Injuries in Soccer: A Prospective Study Using Muscle Functional Magnetic  
716 Resonance Imaging. *Am J Sports Med* 2016.
- 717 36. **Seymore KD, Domire ZJ, DeVita P, Rider PM, and Kulas AS.** The effect of Nordic  
718 hamstring strength training on muscle architecture, stiffness, and strength. *Eur J Appl Physiol*  
719 117: 943-953, 2017.
- 720 37. **Spoor CW, and van Leeuwen JL.** Knee muscle moment arms from MRI and from  
721 tendon travel. *J Biomech* 25: 201-206, 1992.



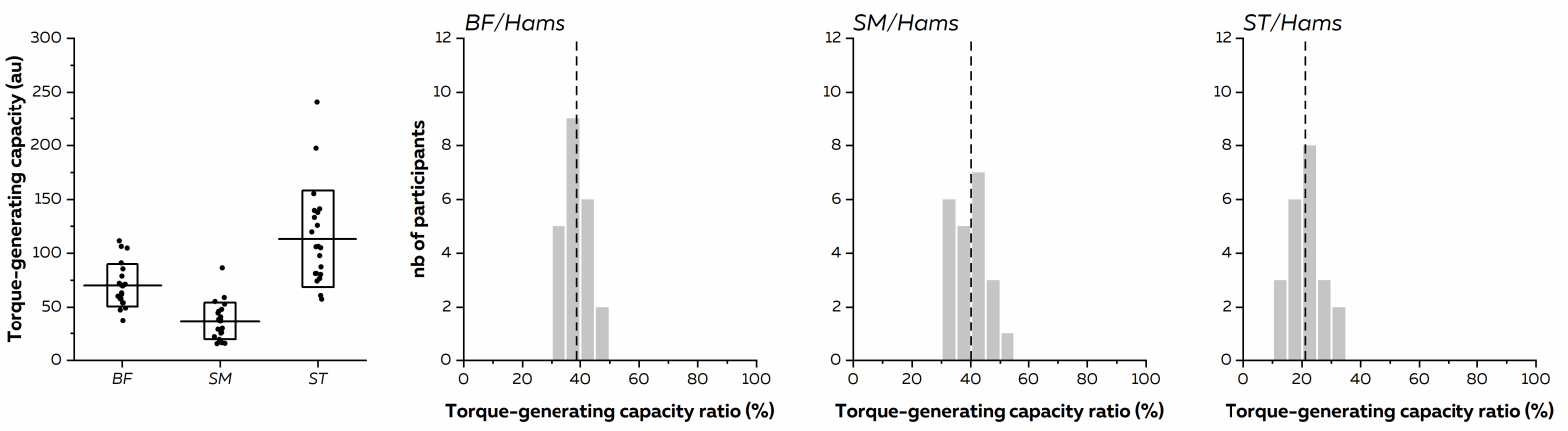
- 722 38. **Todd G, Taylor JL, and Gandevia SC.** Reproducible measurement of voluntary  
723 activation of human elbow flexors with motor cortical stimulation. *J Appl Physiol* (1985) 97:  
724 236-242, 2004.
- 725 39. **Tsianos GA, Rustin C, and Loeb GE.** Mammalian muscle model for predicting force  
726 and energetics during physiological behaviors. *IEEE Trans Neural Syst Rehabil Eng* 20: 117-  
727 133, 2012.
- 728 40. **van Ingen Schenau GJ, Dorssers WM, Welter TG, Beelen A, de Groot G, and**  
729 **Jacobs R.** The control of mono-articular muscles in multijoint leg extensions in man. *J*  
730 *Physiol* 484 ( Pt 1): 247-254, 1995.
- 731 41. **Visser JJ, Hoogkamer JE, Bobbert MF, and Huijing PA.** Length and moment arm  
732 of human leg muscles as a function of knee and hip-joint angles. *Eur j appl physiol occup*  
733 *physiol* 61: 453-460, 1990.
- 734 42. **Ward SR, Eng CM, Smallwood LH, and Lieber RL.** Are current measurements of  
735 lower extremity muscle architecture accurate? *Clin Orthop Relat Res* 467: 1074-1082, 2009.
- 736 43. **Wickiewicz TL, Roy RR, Powell PL, and Edgerton VR.** Muscle Architecture of the  
737 Human Lower Limb. *Clin Orthop Relat Res* 179: 275-283, 1983.
- 738 44. **Woodley SJ, and Mercer SR.** Hamstring muscles: architecture and innervation. *Cells*  
739 *Tissues Organs* 179: 125-141, 2005.
- 740

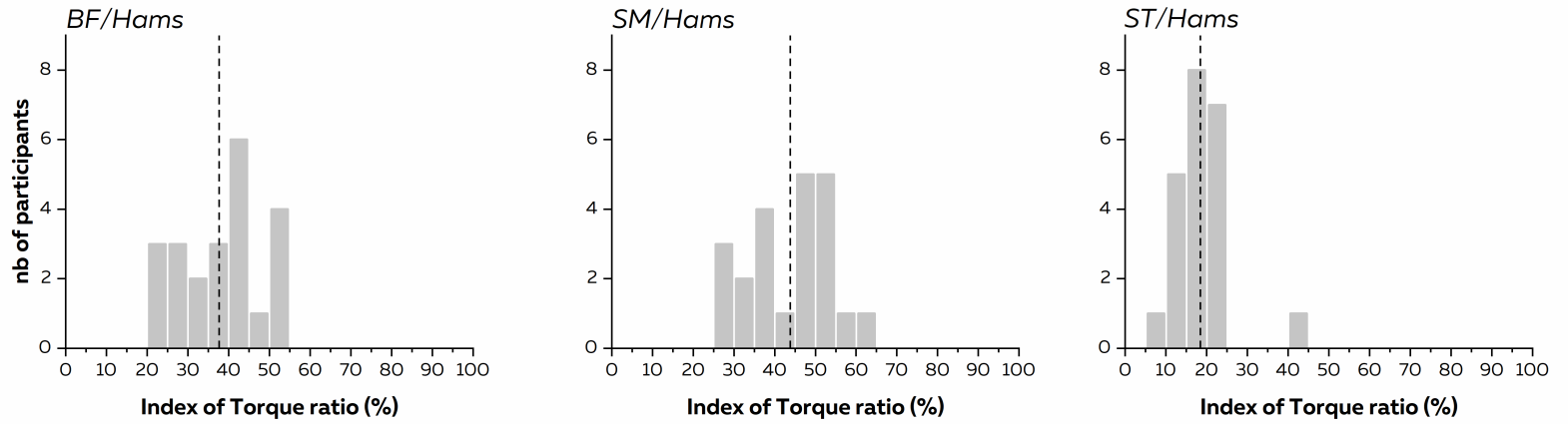


# A Muscle activation



# B Torque-generating capacity



**A****B**